PUBLICATIONS OF THE ASTRONOMICAL SOCIETY OF THE PACIFIC
100: 1134–1151, September 1988

JHKLM PHOTOMETRY: STANDARD SYSTEMS, PASSBANDS, AND INTRINSIC COLORS

M. S. BESSELL AND J. M. BRETT

Mount Stromlo and Siding Spring Observatories, Australian National University, Private Bag, P.O. Woden, ACT 2606, Canberra, Australia

Received 1987 March 1, revised 1988 May 2

ABSTRACT

The relations between colors of the *JHKL* systems of SAAO (Glass *et al.*), ESO (Engels *et al.*; Wamsteker), CIT/CTIO (Elias *et al.*), MSO (Jones and Hylund; Hylund andMcGregor), AAO (Allen *et al.*), and Arizona (Johnson *et al.*) have been examined and linear relations derived to enable transformation between the $(J-K)$, $(J-H)$, $(H-K)$, and $(K-L)$ colors in the different systems. A homogenized system, essentially the Johnson-Glass system, is proposed and its absolute calibration derived based on the Bell model-atmosphere fluxes for α Lyr. The homogenized colors of the standard stars were used to derive intrinsic colors for stars with spectral types between B7 V and M6 V and G7 III and M5 III. The *JHKL* passbands of the MSO IR system, derived from measured filter passbands and estimated atmospheric transmission values, were used to compute synthetic colors from relative absolute fluxes of some stars (including the Sun). The reasonable agreement with the standardized *JHKL* colors indicates that these passbands can be adopted as representing the homogeneous system and used to compute broad-band IR colors from theoretical or observed fluxes. The passbands of other IR systems were similarly estimated from published data, and the synthetic colors were intercompared using blackbody and stellar fluxes. These passbands were then adjusted in wavelength to produce agreement with the observed relations between different systems, enabling the effective wavelengths of the different natural systems to be estimated. Better effective wavelength could be determined were spectrophotometry available for the very red stars with known broad-band colors.

Key words: photometry–infrared photometric transformations–infrared passbands–infrared intrinsic colors

I. Introduction

Scholz (1985) and Bessell *et al.* (1985, 1988*a,b*) have computed extended model atmospheres relevant to KM giants and Mira variables. Brett (1988) has examined the detailed molecular opacities for these models and synthetic spectra have been produced from which we intend to derive broad-band *JHKL* colors for comparison with the extensive published photometry. Unfortunately, many natural *JHKL* photometric systems exist and, although they have common ancestory in the *JKLM* "Johnson" system of Johnson *et al.* (1966) and *JHKL* system of Glass (1974), and in their InSb detectors, the filters are not identical. Standardization has mainly involved adoption of zero points based on zero colors for an average "A0" star or for Vega and not adjustment for any differences in the filter effective wavelengths. The *J* passbands in particular are known to differ between the MSO, AAO, CIT/CTIO, and Johnson systems; however, when we computed synthetic IR colors using measured filter passbands for the MSO system it was apparent that the *J* band was *not* at the effective wavelength inferred from published comparisons of the various systems. Arbitrarily shifting the passband to the red helped somewhat, but the shift was far greater than could be justified by any uncertainties, such as atmospheric cutoff. Similar difficulties were encountered when computing colors for published passbands of other systems. Clearly we needed to reexamine the basis of passband and effective wavelength derivations.

Koornneef (1983*a*) had previously analyzed the photometry of the SAAO, ESO, AAO, and Johnson systems and produced a homogenized system of *JHKLM* magnitudes (Koornneef 1983*b*). However, as most observers tend to publish *K* magnitudes and colors relative to that magnitude, such as $(J-K)$, $(H-K)$, and $(K-L)$, it is better to analyze intercomparisons in this way. But in addition to the data avilable to Koornneef, we now have a more extensive list of MSO standards (Hyland and McGregor 1986) containing many M dwarfs, the comparison of the AAO and CIT/CTIO systems (Elias *et al.* 1983), some L' and *M* standards of MKO (Sinton and Tittemore 1984), and the important review of Glass (1985).

In this paper, we discuss the intercomparisons between colors measured in different systems for common stars, and also examine the mean relations between "pure" IR colors (in the different systems) such as $(J-K)$, $(H-K)$, and $(K-L)$ and the "mixed" color $(V-K)$ and the near-IR color $(V-I)$ of the Kron-Cousins system. The $(V-I)$ colors were obtained from Cousins (1980*a*,*b*), with additional M-dwarf colors from Bessell (1988*a*). This enabled us to use measurements for more stars than those in common and derive independent zero-point corrections.

The published photometric lists were combined using linear transformations and mean $(J-H)$, $(H-K)$, $(J-K)$, $(K-L)$, and $(K-M)$ versus $(V-K)$ and $(V-I)$ regressions derived for giant and dwarf stars. These mean colors are presented in tables for the various spectral classes. For giant stars we adopted the spectral-type versus $(V-K)$ relation of Ridgway *et al.* (1980). The $(V-I)$ versus spectral-type relation for earlier giant stars was derived using photometry from Cousins (1980*a*,*b*) and spectral types from Houk and Cowley (1975) and Houk (1978, 1982). The spectral-type versus $(V-K)$ and $(V-I)$ relations for M dwarfs were taken from Bessell (1988*b*) and Boeshaar (1976).

Finally, we discuss the passbands of the MSO system, for which we have the most information, and compare these with passbands of the other major systems by intercomparing blackbody colors and colors from observed spectra of some KM giants. In most cases it was necessary to shift the passbands in effective wavelength to produce near agreement with the observed linear relations between the different system colors and those of the MSO system. The adopted MSO passbands appear to reasonably reproduce the "standard" homogenized colors and so can be used to compute broad-band colors from IR spectra or model-atmosphere fluxes.

II. The $(V-K)$ Colors and the K Magnitudes

The relation between the different K magnitudes has been examined in three ways: by direct comparison of K magnitudes, or by comparison of $(V-K)$ colors, and by comparison of the $(V-K)$ versus $(V-I)$ relations. In analyzing the relation between colors in widely separated wavelengths we have tried to remove reddened stars and binary stars from the comparisons. The results for the common $(V-K)$ data are

$$
\begin{array}{lclclll}
(V-K)_{SAAO} & = & 0.013(\pm 0.007) & + & 0.993(\pm 0.003)\ (V-K)_J & \text{s.d. } 0.034 & 87 \text{ stars} \\
(V-K)_{ESO} & = & -0.017(\pm 0.018) & + & 0.999(\pm 0.009)\ (V-K)_{SAAO} & \text{s.d. } 0.036 & 19 \text{ stars} \\
(V-K)_{AAO} & = & 0.004(\pm 0.008) & + & 0.998(\pm 0.007)\ (V-K)_{SAAO} & \text{s.d. } 0.027 & 21 \text{ stars} \\
(V-K)_{AAO} & = & -0.003(\pm 0.005) & + & 0.994(\pm 0.002)\ (V-K)_{MSO} & \text{s.d. } 0.018 & 27 \text{ stars} \\
(V-K)_{CIT} & = & 0.014(\pm 0.013) & + & 1.000(\pm 0.002)\ (V-K)_{AAO} & \text{s.d. } 0.021 & 21 \text{ stars}\ .
\end{array}
$$

Assuming that the V magnitudes are the same, these relations reflect the following differences in the K magnitudes.

$$
\begin{array}{lclclcl}
K_J & = & K_{SAAO} & + & 0.013(\pm 0.007) & - & 0.007(\pm 0.003)\ (V-K) \\
K_{ESO} & = & K_{SAAO} & + & 0.017(\pm 0.018) & + & 0.001(\pm 0.009)\ (V-K) \\
K_{AAO} & = & K_{SAAO} & - & 0.004(\pm 0.008) & + & 0.002(\pm 0.007)\ (V-K) \\
K_{CIT} & = & K_{SAAO} & - & 0.014(\pm 0.013) & + & 0.000(\pm 0.002)\ (V-K)
\end{array}
$$

Apart from the relation between K_J and K_{SAAO} these are very similar to those derived by Glass (1985).

The $(V-K)$ versus $(V-I)$ relations are not exactly linear (9th order gave good fits) but are useful for indicating the precision of the $(V-K)$ data and the zero points (zp) of the $(V-K)$ color. The following zero points are the values of $(V-K)$ when $(V-I) = 0$.

SAAO	$(V-K)$ versus $(V-I)$	zp $0.010(\pm 0.010)$	s.d. 0.037	128 stars
Johnson	$(V-K)$ versus $(V-I)$	zp $-0.028(\pm 0.018)$	s.d. 0.048	82 stars
ESO	$(V-K)$ versus $(V-I)$	zp $-0.021(\pm 0.016)$	s.d. 0.033	60 stars
AAO	$(V-K)$ versus $(V-I)$	zp $0.024(\pm 0.014)$	s.d. 0.037	53 stars
MSO	$(V-K)$ versus $(V-I)$	zp $0.010(\pm 0.013)$	s.d. 0.039	46 stars

These comparisons indicate that all the systems have similar precision (± 0.04) in their $(V-K)$ colors but that the zero points for the $(V-K)$ colors of the various systems need slight adjustment; however, the direct $(V-K)$ comparisons show a smaller scatter in $(V-K)$ and smaller zero points. It is probable that intrinsic scatter in the $(V-I)$, $(V-K)$ relation is responsible for part of this discrepancy, but it is also likely that the smaller scatter in the $(V-K)$ correlations results from their common ancestry.

Elias, Frogel, and Humphreys (1985) have also compared CIT and Johnson K magnitudes, and from that paper one can deduce that $K_J - K_{CIT} \approx 0.05 - 0.015\,(V-K)$, with a scatter of ± 0.04, although the relation clearly was not linear. Second-order curves were also better fits to most of our $(V-K)$ comparisons. Nevertheless, given the uncertainties involved in all these comparisons we will adopt the following linear relations in combining the systems.

$$(V-K) = -0.005 + (V-K)_{SAAO} \qquad (V-K) = 0.01 + 0.993\ (V-K)_J$$
$$(V-K) = 0.015 + (V-K)_{ESO} \qquad (V-K) = -0.012 + 0.997\ (V-K)_{MSO}$$
$$(V-K) = 0.00 + 1.002\ (V-K)_{AAO} \qquad (V-K) = -0.02 + 1.001\ (V-K)_{CIT}$$

In Figures 1 to 5 we present the combined data of Glass (1974) (SAAO), Engels *et al.* (1981) and Wamsteker (1981) (ESO), Allen and Cragg (1983) (AAO), Hyland and McGregor (1986) (MSO), Elias *et al.* (1982) (CIT), Lee (1970), Johnson, MacArthur, and Mitchell (1968) (Johnson), Persson, Aaronson, and Frogel (1977) (PAF), and Stauffer and Hartman (1986) (SH). In Figure 1 the sequence bifurcates near a $(V-K)$ value of 3.3 due to the appearance of TiO bands. The lower sequence refers to the giant stars. The SAAO, ESO, and Lee data, being only of bright stars, provides most of the data for the KM giant sequence, while the MSO, CIT, AAO, PAF, and SH data provide the data for the KM dwarf sequence. Giants and supergiants are plotted as plus signs, dwarfs as filled squares.

III. The $(J-K)$ Colors

From the published data lists discussed above, the following relations were derived.

$$(J-K)_{SAAO} = -0.001(\pm0.005) + 0.996(\pm0.005)\ (J-K)_J \quad \text{s.d. } 0.026 \quad 85 \text{ stars, } (J-K) < 1.2$$
$$(J-K)_{ESO} = 0.009(\pm0.019) + 0.974(\pm0.034)\ (J-K)_{SAAO} \quad \text{s.d. } 0.037 \quad 19 \text{ stars, } (J-K) < 1.1$$
$$(J-K)_{AAO} = 0.004(\pm0.005) + 1.044(\pm0.009)\ (J-K)_{SAAO} \quad \text{s.d. } 0.019 \quad 21 \text{ stars, } (J-K) < 0.8$$
$$(J-K)_{MSO} = -0.004(\pm0.004) + 0.956(\pm0.008)\ (J-K)_{AAO} \quad \text{s.d. } 0.017 \quad 31 \text{ stars, } (J-K) < 1.1$$
$$(J-K)_{CIT} = 0.006(\pm0.005) + 0.897(\pm0.004)\ (J-K)_{AAO} \quad \text{s.d. } 0.018 \quad 21 \text{ stars, } (J-K) < 3.0$$

Glass (1983, 1985) has also published similar relations, including analysis of unpublished observations by Carter (1984), who observed with a J filter similar to that of the AAO, and H and K filters similar of SAAO and MSO. The following equations can be derived from Glass's relations.

$$(J-K)_J = 0.000 + 1.008(J-K)_{SAAO} \qquad (J-K)_{ESO} = 0.006 + 0.985(J-K)_{SAAO}$$
$$(J-K)_{AAO} = -0.005 + 1.027(J-K)_{SAAO} \qquad (J-K)_{MSO} = -0.022 + 0.979(J-K)_{SAAO}$$
$$(J-K)_{CIT} = -0.003 + 0.914(J-K)_{SAAO} \qquad (J-K)_{Cart} = -0.004 + 1.026(J-K)_{CIT}$$

(Glass's uncertainties for the AAO and CIT fits are smaller than those we derived above because of his unpublished observations of the very red stars.) As was done for the $(V-K)$ colors above, 9th-order polynomials were also fitted to the $(J-K)$, $(V-I)$ colors. The zero points and standard deviations were:

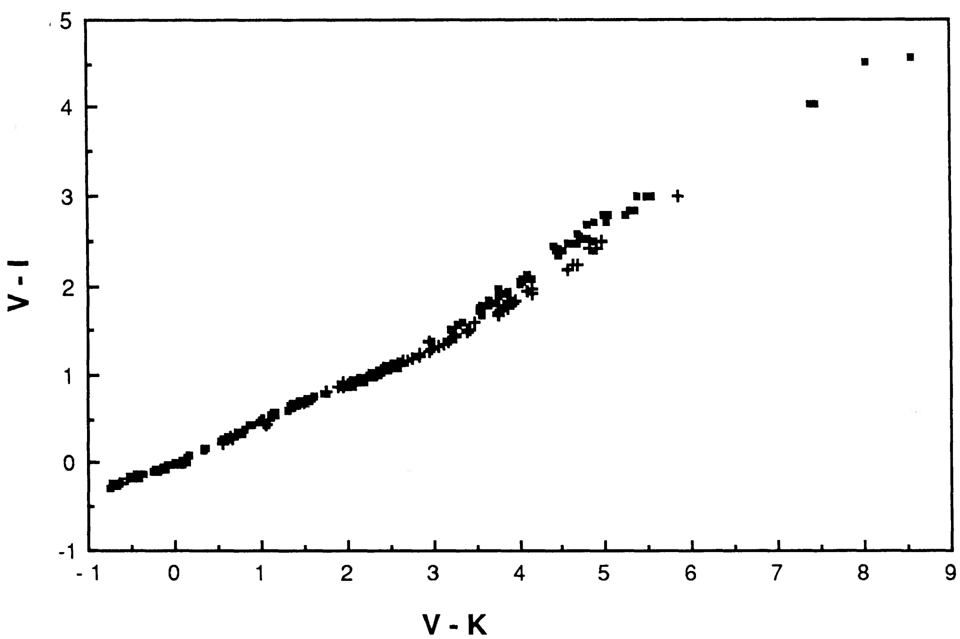

FIG. 1–$(V-K)$ versus $(V-I)$ diagram. Combined data from Glass (1974), Engels *et al.* (1981), Wamsteker (1981), Allen and Cragg (1983), Hyland and McGregor (1986), Elias *et al.* (1982), Lee (1970), Johnson *et al.* (1968), Persson, Aarsonson, and Frogel (1977), and Stauffer and Hartman (1986). Giants and supergiants +, dwarfs ■.

	SAAO	Johnson	ESO	AAO	MSO
zp	0.005(±0.006)	−0.002(±0.011)	0.030(±0.014)	0.007(±0.007)	0.005(±0.012)
s.d.	0.023	0.029	0.042	0.020	0.020 .

We decided to adopt as the standard $(J-K)$ scale, the scale close to that of Johnson, SAAO, ESO, and MSO, although the redder J filter of CIT, which almost completely avoids the H_2O band near 1.12 microns thus permitting more accurate photometry, would have been a better initial choice. The J filter of Carter and the AAO which extends further to the blue is the most affected by the atmospheric water and is not as good.

We propose the following transformations to a homogeneous system.

$$(J-K) = -0.005 + (J-K)_{SAAO} \qquad (J-K) = 0.01 + 0.99\ (J-K)_J$$
$$(J-K) = -0.010 + 1.025\ (J-K)_{ESO} \qquad (J-K) = 0.010 + 1.008\ (J-K)_{MSO}$$
$$(J-K) = 0.0 + 0.974\ (J-K)_{AAO} \qquad (J-K) = -0.002 + 1.086\ (J-K)_{CIT}.$$

In Figure 2 the combined data are shown. The bifurcation between KM giants and dwarfs is clearly shown; most of the scatter in the lower dwarf sequence is the effect of metallicity variation among the dwarfs.

IV. The $(H-K)$ Colors

The $(H-K)$ colors of most stars in the lists do not change much with temperature; hence, it is more difficult to see the effects of the H-bandpass mismatches given the observational imprecision of the data and the small $(H-K)$ differences between A and K stars. A good test is to observe heavily reddened stars as done by Elias *et al.* (1983) for the AAO/CIT comparison and Glass (1983) for the SAAO/CIT and SAAO/AAO comparisons. One must be aware, however, that the H^--opacity minimum and the H_2O absorption produces energy distributions in late-type stars that differ from the smooth spectra of blackbodies and reddened early-type stars, and systematically different relations could be derived for these different objects. The following relations were evident from our comparisons.

$$(H-K)_{AAO} = -0.001(\pm0.003) + 0.982(\pm0.018)\ (H-K)_{MSO} \quad \text{s.d. } 0.010 \quad 27 \text{ stars}, (H-K) < 0.30$$
$$(H-K)_{CIT} = -0.002(\pm0.004) + 0.954(\pm0.010)\ (H-K)_{AAO} \quad \text{s.d. } 0.014 \quad 21 \text{ stars}, (H-K) < 0.90$$
$$(H-K)_{ESO} = -0.017(\pm0.014) + 1.134(\pm0.129)\ (H-K)_{SAAO} \quad \text{s.d. } 0.026 \quad 17 \text{ stars}, (H-K) < 0.20$$

From Glass (1983, 1985) we can also derive

$$(H-K)_{ESO} = -0.013 + 1.30\ (H-K)_{SAAO} \qquad (H-K)_{CIT} = -0.017 + 0.986(H-K)_{SAAO}$$
$$(H-K)_{MSO} = -0.043 + 0.961\ (H-K)_{SAAO} \qquad (H-K)_{AAO} = -0.015 + 1.016(H-K)_{SAAO}\ .$$

Although the original Johnson catalog (Johnson *et al.* 1966) did not contain H measurements, photometry of Johnson

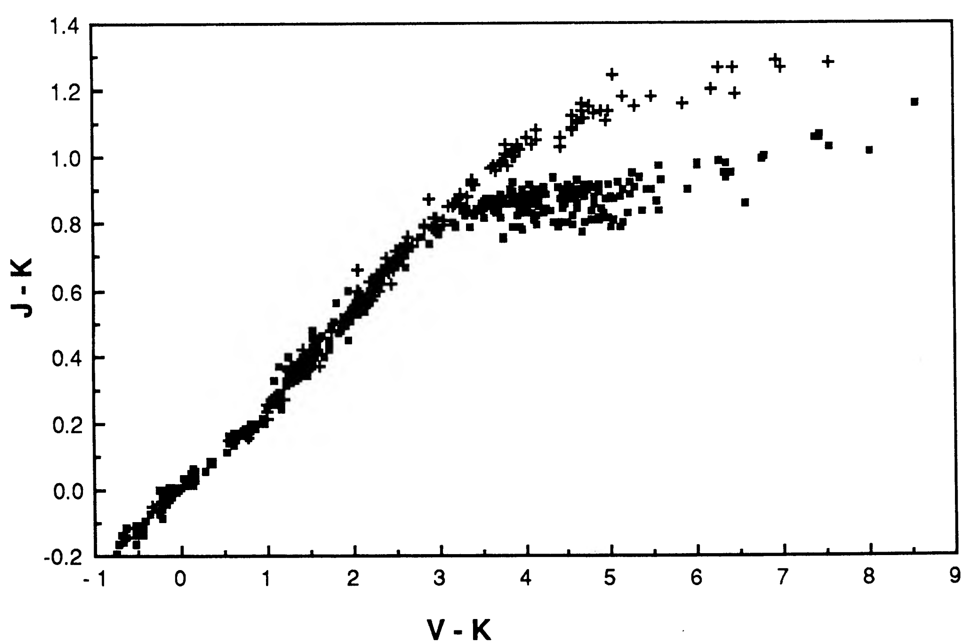

FIG. 2–$(J-K)$ versus $(V-K)$ diagram. Combined data, see caption Figure 1.

et al. (1968) and Lee (1970) did include H photometry. We adopt the bright giants and other better measured stars from these lists to define $(H-K)$ and $(J-H)$ colors in the Johnson system. Elias *et al.* (1985) give from 13 stars in common with the two data sets

$$(H-K)_{\mathrm{CIT}} = -0.009(\pm 0.017) + 0.912(\pm 0.059)\ (H-K)_{\mathrm{J}}\ .$$

In agreement with this result we found that the $(V-K)_{\mathrm{J}}$ versus $(H-K)_{\mathrm{J}}$ diagram from that data was the same (within the scatter) as the diagram from the Glass sample. There were insufficient early-type stars to define a zero point. To obtain more reliable transformations between the ESO and Johnson systems and those of SAAO, AAO, MSO, and CIT, it is imperative that comparisons across a longer $(H-K)$ baseline be made by using the ESO and Johnson filters to observe the very red stars of Elias *et al.* (1983).

Relations between $(H-K)$ and $(V-I)$ were also examined. The following zero points and standard deviations were derived.

	SAAO	ESO	AAO	MSO
zp	0.021(±0.005)	0.007(±0.007)	0.005(±0.003)	0.012(±0.006)
s.d.	0.019	0.021	0.005	0.018

The $(H-K)$ systems are therefore very similar, except for ESO whose H passband appears too far to the blue. Adopting the original SAAO scale as the standard, we suggest the following transformations.

$$(H-K) = -0.021 + (H-K)_{\mathrm{SAAO}} \qquad (H-K) \approx 0.01 + 0.91\ (H-K)_{\mathrm{J}}$$
$$(H-K) = 0.005 + 0.87\ (H-K)_{\mathrm{ESO}} \qquad (H-K) = -0.007 + 0.97\ (H-K)_{\mathrm{MSO}}$$
$$(H-K) = -0.003 + 0.98\ (H-K)_{\mathrm{AAO}} \qquad (H-K) = 0.0 + 1.03\ (H-K)_{\mathrm{CIT}}$$

Figure 3 shows the combined data; the ESO stars provide the larger scatter. The bifurcation between the M giants and dwarfs is evident for the reddest stars, the dwarfs being redder in $(H-K)$ for a given $(V-K)$.

V. The $(J-H)$ Colors

Although this color can be derived from $(J-K)$ and $(H-K)$, it is commonly considered separately. We derived the following relations.

$$(J-H)_{\mathrm{ESO}} = 0.037(\pm 0.015) + 0.926(\pm 0.033)\ (J-H)_{\mathrm{SAAO}} \qquad \text{zp } 0.031 \qquad 19 \text{ stars}$$
$$(J-H)_{\mathrm{AAO}} = 0.013(\pm 0.004) + 1.050(\pm 0.016)\ (J-H)_{\mathrm{SAAO}} \qquad \text{zp } 0.014 \qquad 22 \text{ stars}$$
$$(J-H)_{\mathrm{AAO}} = 0.011(\pm 0.003) + 1.056(\pm 0.009)\ (J-H)_{\mathrm{MSO}} \qquad \text{zp } 0.012 \qquad 29 \text{ stars}$$
$$(J-H)_{\mathrm{AAO}} = -0.015(\pm 0.005) + 1.141(\pm 0.006)\ (J-H)_{\mathrm{CIT}} \qquad \text{zp } 0.016 \qquad 21 \text{ stars}$$

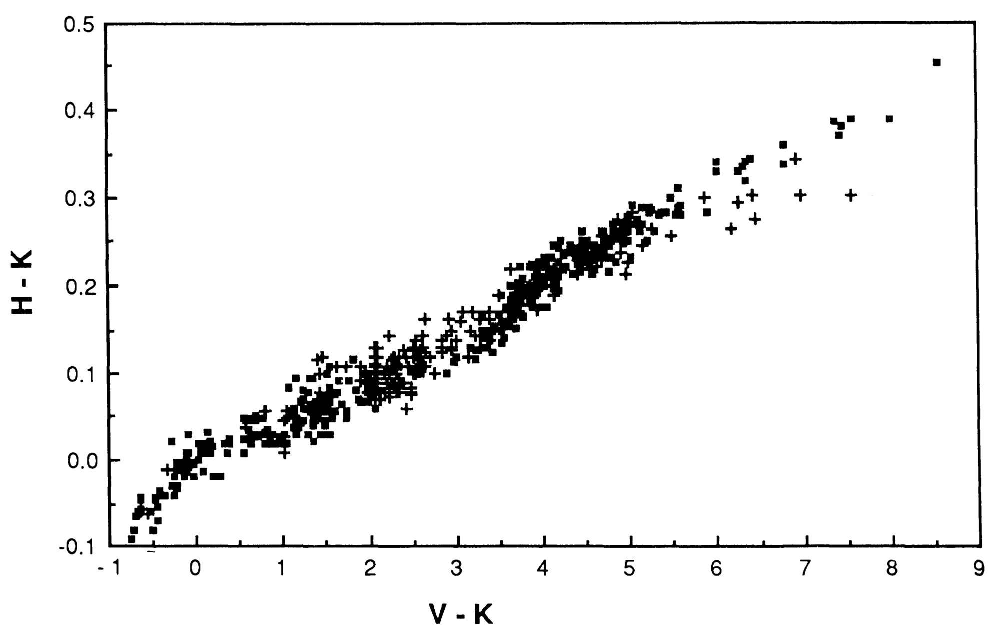

FIG. 3–$(H-K)$ versus $(V-K)$ diagram. Combined data, see caption Figure 1.

Although there were no stars in common between the lists of Glass and those of Lee (1970) and Johnson *et al.* (1968), from comparison of the Glass and Johnson $(J-H)$ versus $(V-K)$ diagrams one could derive

$$(J-H)_{\rm Glass} \approx -0.02 + 1.01\,(J-H)_{\rm J}\ .$$

From Glass (1983, 1985) we derived

$$\begin{array}{lllllllllll}
(J-H)_{\rm ESO} & = & 0.043 & + & 0.91 & (J-H)_{\rm SAAO} & \qquad (J-H)_{\rm CIT} & = & 0.015 & + & 0.918\ (J-H)_{\rm SAAO} \\
(J-H)_{\rm AAO} & = & 0.015 & + & 1.047 & (J-H)_{\rm SAAO} & \qquad (J-H)_{\rm MSO} & = & & + & 0.994\ (J-H)_{\rm SAAO}\ .
\end{array}$$

The $(V-I)$ versus $(J-H)$ regressions provided the following zero points and standard deviations.

	SAAO	ESO	AAO	MSO
zp	−0.016(±0.006)	0.021(±0.011)	0.003(±0.008)	−0.011(±0.016)
s.d.	0.022	0.03	0.024	0.024

The following transformations are suggested.

$$\begin{array}{llllll}
(J-H) & = & 0.016 & + & & (J-H)_{\rm SAAO} \\
(J-H) & = & -0.028 & + & 1.105 & (J-H)_{\rm ESO} \\
(J-H) & = & 0.005 & + & 0.963 & (J-H)_{\rm AAO}
\end{array}
\qquad
\begin{array}{llllll}
(J-H) & = & -0.004 & + & 1.01 & (J-H)_{\rm J} \\
(J-H) & = & 0.017 & + & 1.016 & (J-H)_{\rm MSO} \\
(J-H) & = & 0.002 & + & 1.098 & (J-H)_{\rm CIT}
\end{array}$$

Figure 4 and Figure 5 show the combined data. As in the $(J-K)$ diagram the bifurcation between M giants and M dwarfs is clear. The scatter evident in the M dwarfs is probably due to metallicity variations.

VI. The $(K-L)$ Colors

The increasing brightness of the background and the higher atmospheric absorption makes photometry at longer wavelengths than K more difficult, especially from the ground. This is reflected in the higher scatter in the published $(K-L)$ colors, compared to $(J-K)$ or $(H-K)$. We examined, for the different systems, the relations between $(K-L)$ and $(V-I)$ and $(V-K)$. These generally were adequately fitted with the following linear relations.

$$\begin{array}{lllllllll}
\text{SAAO} & (K-L) & = & -0.001(\pm0.007) & + & 0.038(\pm0.003) & (V-K) & \text{s.d. } 0.046 & \text{126 stars} \\
\text{ESO} & (K-L) & = & 0.032(\pm0.005) & + & 0.038(\pm0.002) & (V-K) & \text{s.d. } 0.029 & \text{77 stars} \\
\text{Johnson} & (K-L) & = & 0.027(\pm0.008) & + & 0.040(\pm0.003) & (V-K) & \text{s.d. } 0.054 & \text{130 stars (non-late M)} \\
\text{Wamsteker} & (K-L) & = & 0.016(\pm0.006) & + & 0.039(\pm0.003) & (V-K) & \text{s.d. } 0.012 & \text{11 stars} \\
\text{CIT} & (K-L) & = & -0.010(\pm0.009) & + & 0.039(\pm0.005) & (V-K) & \text{s.d. } 0.015 & \text{11 stars (non-M)} \\
 & & = & -0.013(\pm0.011) & + & 0.033(\pm0.008) & (V-K) & \multicolumn{2}{l}{+\ 0.0026(\pm0.0011)\ (V-K)^2}
\end{array}$$

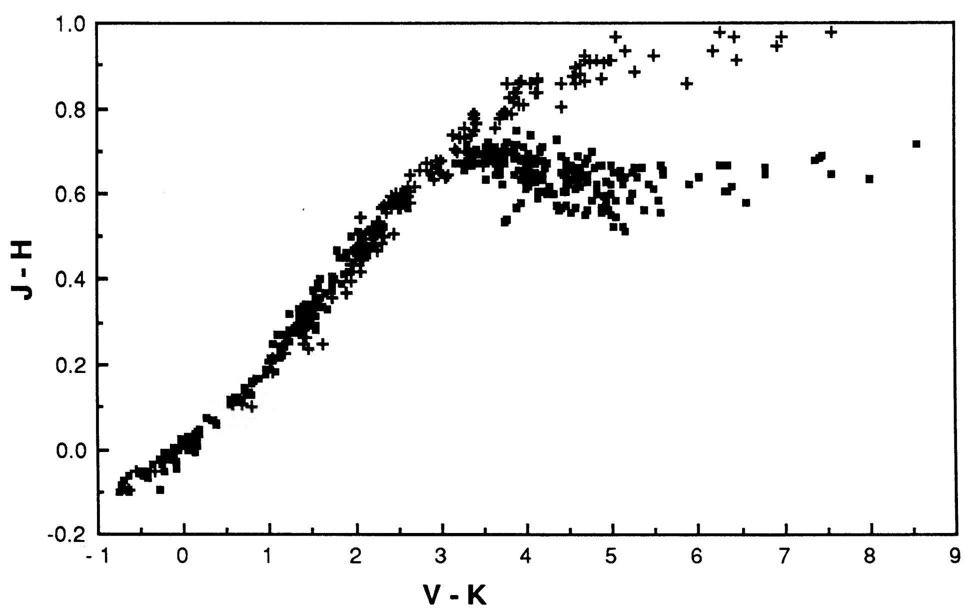

FIG. 4–$(J-H)$ versus $(V-K)$ diagram. Combined data, see caption Figure 1.

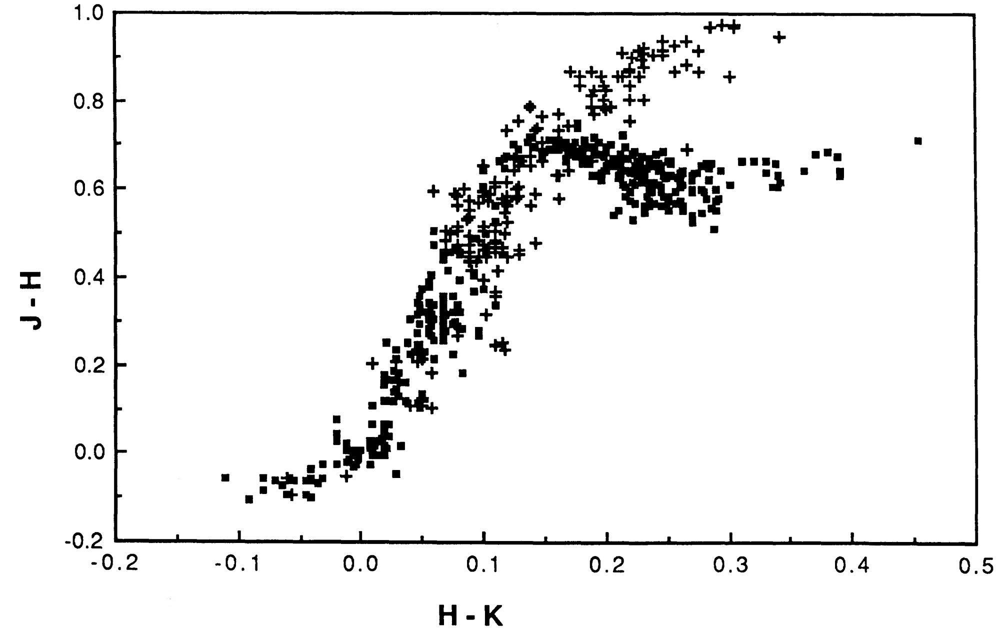

FIG. 5–$(J-H)$ versus $(H-K)$ diagram. Combined data, see caption Figure 1.

The more precise CIT data show clearly that the regression is not linear, $(K-L)$ changing more quickly with $(V-K)$ for the B and M stars than for the A to K stars. As well as one can judge, given the generally large scatter, the effective wavelengths of the $(K-L)$ systems are very similar. The data of Wamsteker and CIT are of higher precision than the others.

The AAO L' (3.8 μ; 3.55 μ to 4.15 μ) system, however, is different. Its L' filter was chosen to be redder than the original L filter (3.5 μ) of Johnson, thus avoiding the worst of the atmospheric absorption, and although it is more affected by thermal background, its adoption as the standard should be encouraged, at least for low-altitude observations. The original red cutoff in the L response was determined by the PbS detector sensitivity falloff and the blueward cutoff was set to maximize the throughput; but now that InSb is the usual detector the only point in persisting with a bluer L band, which is badly affected by the atmospheric water, is because of the lower thermal background. The high precision of the CIT observations shows, however, that accurate photometry is possible with the bluer filter, at least from a dry site. The L' (3.45 μ to 4.10 μ) system of Sinton and Tittemore (1984) (Mauna Kea Observatory) appears similar to that of the AAO as seen from the $(K-L')$ versus $(V-K)$ plot of colors of stars common to the CIT and MKO standard lists, but the passbands do not exactly match. Mount Stromlo may have obtained a similar L' filter which produces a bandpass from 3.40 μ to 4.15 μ, and we have computed synthetic colors with this filter also.

The $(K-L)$ versus $(V-K)$ plot of CIT and the $(K-L')$ versus $(V-K)$ plot of AAO can be brought into good agreement with the transformation

$$(K-L')_{\mathrm{AAO}} = 1.33\,(K-L)_{\mathrm{CIT}}\ , \qquad \text{for } -1 < (V-K) < 6\ ;$$

but one should be aware that H_2O absorption in M-type Miras, M dwarfs, and giant M stars with spectral types later than M5 affects L much more than L' and that a transformation valid for A to K stars will not work for late-M giants or M dwarfs.

Glass (1985) analyzed $(K-L)$ colors relative to those of Carter and from his relations one could deduce that there were significant differences between the different systems. However, the uncertainties in his relations were high because of the imprecision in much of the data and because there were few stars in common for some of the comparisons. In addition, as noted above, the H_2O absorption in M stars produces differences between giants and dwarfs and differences due to L-filter mismatches; consequently, comparisons may give different results depending on whether M stars are included or excluded and whether the M stars are giants or dwarfs. Given the accuracy of the *existing* $(K-L)$ photometry, it is reasonable to assume that all L (3.5 μ) systems are identical to that of CIT and to adopt that scale as the 3.5 μ standard. We adopt the AAO L' (3.8 μ) system as standard but note that a small color correction should be required to bring the L' systems of MKO and MSO into exact agreement with this. The following relations are suggested.

$(K-L)$	$=$	0.0	$+$	$(K-L)_{SAAO}$	$(K-L)$	$=$	-0.03	$+ (K-L)_{J}$
$(K-L)$	$=$	-0.03	$+$	$(K-L)_{ESO}$	$(K-L)$	$=$	-0.02	$+ (K-L)_{WAM}$
$(K-L)$	$=$	-0.02	$+$	$(K-L)_{MSO}$	$(K-L)$	$=$	0.0	$+ (K-L)_{CIT}$
$(K-L')$	$=$	0.0	$+$	$(K-L')_{AAO}$	$(K-L')$	$=$	0.0	$+ 1.04\ (K-L')_{MKO}$

In Figure 6(a) the $(K-L)$ data of CIT are shown. Figure 6(b) shows the $(K-L')$ data of the AAO. There are few late-M giants in the standard lists of precise photometry; however, the M dwarfs and M giants have systematically different $(K-L)$ colors. This results from the stronger absorption bands of H_2O in the L and L' band of dwarfs compared to giants of the same $(V-K)$ color. Although the L' passbands of MKO and MSO are not identical to that of the AAO, they do avoid most of the atmospheric absorption and should produce as accurate photometry, but they will produce slightly different colors for late-M stars. The published $(K-L)$ photometry for many of the systems is of lower accuracy than for the J, H, and K colors, and even for the better observed systems the $(K-L)$ data for M dwarfs are also of lower precision because of the relative faintness of dwarfs compared to giants. Therefore, the comparison between systems is weakest for the $(K-L)$ color and requires that care be taken in transforming the colors of M stars between systems until the L passbands of the various systems are better understood.

VII. The $(K-M)$ Colors

The $(K-M)$ photometry is that of ESO (Engels *et al.* 1981; Wamsteker 1981), MKO (Sinton and Tittemore 1984), and

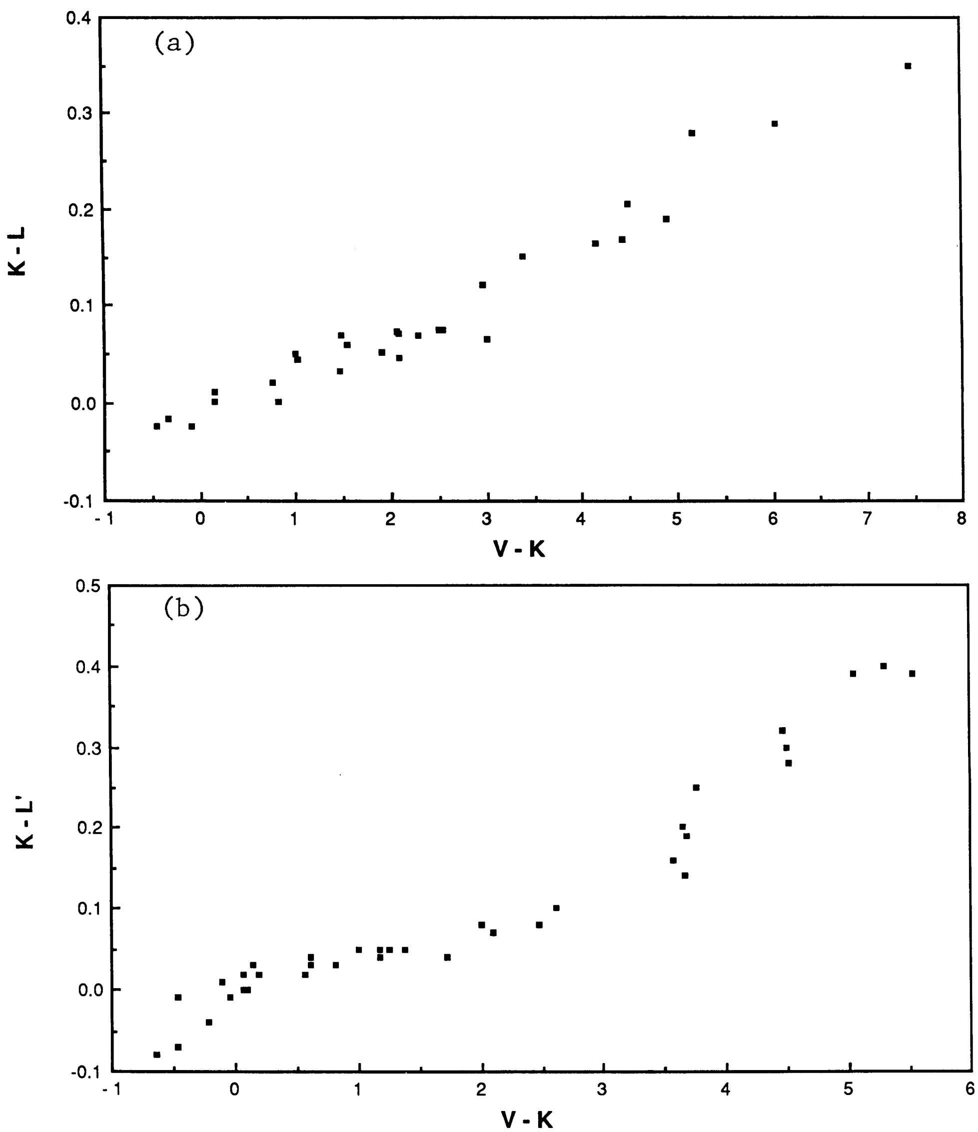

FIG. 6–(a) $(K-L)$ versus $(V-K)$ diagram from Elias *et al.* (1982). (b) $(K-L')$ versus $(V-K)$ diagram from Allen and Cragg (1983).

Thomas, Hyland, and Robinson (1973, THR). In Figure 7 is shown the relation between the $(K-M)$ and $(V-K)$. The bolometer measurements of THR are shown as crosses. The fainter G dwarfs of ESO are not plotted. The stars with the $(K-M)$ colors larger than 0.1 are supergiants as are some of the M stars near $(V-K) = 5$ which lie above the bulk of the stars. All the colors discussed previously $(V-I)$, $(J-K)$, $(H-K)$, $(K-L)$ increased with increasing $(V-K)$ (or decreasing temperature) as expected for continuum or blackbody colors. However, $(K-M)$ increases initially but then decreases toward cooler temperatures, with a suggestion of a flattening or increase again in the late-M giants. This undoubtedly results from the effect of absorption in the stellar spectrum from the fundamental CO band, which occurs in the M "window" between 4.5 and 5.2 microns, as pointed out by THR.

The AAO has a filter very similar to that at ESO, so the same system would be valid; however, the SAAO (Glass 1974) *M* filter is about 0.3 micron further to the red. Apart from the fact that it is observable with an INSb detector there is little value in *M* photometry; the *M* "window" scarcely exists; *M* is blanketed by CO in all cool stars; $(K-L')$ is a much better temperature indicator for the coolest stars, and the 10-μ photometry is a better indicator of circumstellar emission.

VIII. Adopted Transformations to the Glass-Johnson System

We decided to adopt the system of Glass (with zero-point corrections) as the base system for homogenizing the photometry. This system is closely related to that of Johnson, KPNO, MSO, and (at least for $(J-K)$) ESO. The *H* and *K* filters of CIT and AAO are similar to those of Glass also, whereas the *J* filters of CIT and AAO have longer and shorter effective wavelengths, respectively. Although we have succeeded in combining the published photometry reasonably well, there are still significant uncertainties in the transformations between the systems. The $(H-K)$ transformations for Johnson and ESO are uncertain because no colors for very red stars have been published, and systematic differences in the transformation equations for M giant and M dwarf stars are probable in all colors, in particular $(K-L)$, because of the very different strength of H_2O bands in giant and dwarf stars.

In Table I we list the adopted linear transformations for each of the systems we discussed. In addition, we list transformations to the Carter system (discussed by Glass 1985), the HCO system (at least for M dwarfs) discussed by Persson *et al.* (1977), and the M-dwarf colors of Stauffer and Hartman (1986) (SH). The Carter *J* filter is similar to that of the AAO; the *H* and *K* filters are close to the standard system. From the transformations suggested by Persson *et al.* (1977), the *J*, *H*, and *K* filters of the HCO system are all similar to the standard system. Stauffer and Hartman observed with the natural KPNO system (which appears similar to the adopted standard system) but used CTIO standards which are based on a different natural system. The transformations of the SH colors were derived by comparison of their $(J-H)$, $(H-K)$, and $(J-K)$ versus $(V-K)$ diagrams with those of the combined CTIO, MSO, and AAO dwarf diagrams.

IX. Intrinsic Colors for Giants and Dwarfs

We have used the homogenized data sets discussed above to derive intrinsic colors for giants and dwarfs given in Table II and Table III. For M giant stars we adopted the spectral-type versus $(V-K)$ relation of Ridgway *et al.* (1980); the spectral-type versus $(V-K)$ relation for M dwarfs were taken from Bessell (1986*b*). The spectral type versus $(V-I)$ color

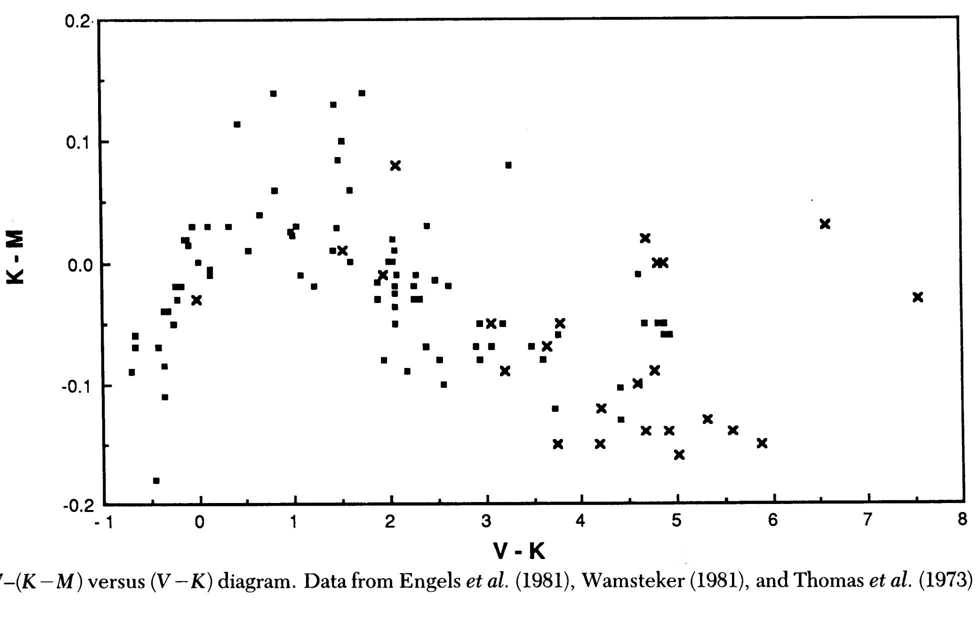

FIG. 7–$(K-M)$ versus $(V-K)$ diagram. Data from Engels *et al.* (1981), Wamsteker (1981), and Thomas *et al.* (1973) (x).

TABLE I

Adopted Linear Transformation Equation Coefficients

	SAAO	Johnson	ESO	MSO	AAO	CIT	Carter	HCO	S&H	Carney
J-H	-0.005	0.01	-0.01	0.01	0.0	-0.002	-0.025	0.00	0.06	0.02
	1.0	1.01	1.105	1.016	0.963	1.098	0.94	1.01	0.97	1.09
H-K	-0.021	0.01:	0.005	-0.007	-0.003	0.00	0.004	0.02	0.005	0.005
	1.0	0.91:	0.87:	0.97	0.98	1.03	0.994	1.0	1.03	1.0
J-K	-0.005	0.01	-0.01	0.01	0.0	-0.002	0.0	0.02	0.05	0.026
	1.0	0.99	1.025	1.008	0.974	1.086	0.975	1.0	1.0	1.073
K-L	0.0	-0.03	-0.03		*	0.0	0.01			
	1.0	1.0	1.0			1.0	0.80:			
V-K	-0.005	0.01	0.015	-0.012	0.0	-0.02	0.005	0.0:	0.0:	0.0:
	1.0	0.993	1.0	0.997	1.002	1.001	1.0	1.0:	1.0:	1.0:

* AAO has a 3.8μ L' filter which defines the K-L' color; MKO has a similar filter and K-L' ≈ 1.04 $(K\text{-}L')_{MKO}$.

TABLE II

Intrinsic Colors for Dwarfs

MK	V-I	V-K	J-H	H-K	J-K	K-L	K-L'	K-M
B8	-0.15	-0.35	-0.05	-0.035	-0.09	-0.03	-0.04	-0.05
A0	0.00	0.00	0.00	0.00	0.00	0.00	0.00	0.00
A2	0.06	0.14	0.02	0.005	0.02	0.01	0.01	0.01
A5	0.27	0.38	0.06	0.015	0.08	0.02	0.02	0.03
A7	0.24	0.50	0.09	0.025	0.11	0.03	0.03	0.03
F0	0.33	0.70	0.13	0.03	0.16	0.03	0.03	0.03
F2	0.40	0.82	0.165	0.035	0.19	0.03	0.03	0.03
F5	0.53	1.10	0.23	0.04	0.27	0.04	0.04	0.02
F7	0.62	1.32	0.285	0.045	0.34	0.04	0.04	0.02
G0	0.66	1.41	0.305	0.05	0.36	0.05	0.05	0.01
G2	0.68	1.46	0.32	0.052	0.37	0.05	0.05	0.01
G4	0.71	1.53	0.33	0.055	0.385	0.05	0.05	0.01
G6	0.75	1.64	0.37	0.06	0.43	0.05	0.05	0.00
K0	0.88	1.96	0.45	0.075	0.53	0.06	0.06	-0.01
K2	0.98	2.22	0.50	0.09	0.59	0.07	0.07	-0.02
K4	1.15	2.63	0.58	0.105	0.68	0.09	0.10	-0.04
K5	1.22	2.85	0.61	0.11	0.72	0.10	0.11	
K7	1.45	3.16	0.66	0.13	0.79	0.11	0.13	
M0	1.80	3.65	0.695	0.165	0.86	0.14	0.17	
M1	1.96	3.87	0.68	0.20	0.87	0.15	0.21	
M2	2.14	4.11	0.665	0.21	0.87	0.16	0.23	
M3	2.47	4.65	0.62	0.25	0.87	0.20	0.32	
M4	2.86	5.26	0.60	0.275	0.88	0.23	0.37	
M5	3.39	6.12	0.62	0.32	0.94	0.29	0.42	
M6	4.18	7.30	0.66	0.37	1.03	0.36	(0.48)	

TABLE III

Intrinsic Colors for Giants (class III)

MK	V-I	V-K	J-H	H-K	J-K	K-L	K-L'	K-M
G0	0.81	1.75	0.37	0.065	0.45	0.04	0.05	0.0
G4	0.91	2.05	0.47	0.08	0.55	0.05	0.06	-0.01
G6	0.94	2.15	0.50	0.085	0.58	0.06	0.07	-0.02
G8	0.94	2.16	0.50	0.085	0.58	0.06	0.07	-0.02
K0	1.00	2.31	0.54	0.095	0.63	0.07	0.08	-0.03
K1	1.08	2.50	0.58	0.10	0.68	0.08	0.09	-0.04
K2	1.17	2.70	0.63	0.115	0.74	0.09	0.10	-0.05
K3	1.36	3.00	0.68	0.14	0.82	0.10	0.12	-0.06
K4	1.50	3.26	0.73	0.15	0.88	0.11	0.14	-0.07
K5	1.63	3.60	0.79	0.165	0.95	0.12	0.16	-0.08
M0	1.78	3.85	0.83	0.19	1.01	0.12	0.17	-0.09
M1	1.90	4.05	0.85	0.205	1.05	0.13	(0.17)	-0.10
M2	2.05	4.30	0.87	0.215	1.08	0.15	(0.19)	-0.12
M3	2.25	4.64	0.90	0.235	1.13	0.17	(0.20)	-0.13
M4	2.55	5.10	0.93	0.245	1.17	0.18	(0.21)	-0.14
M5	3.05	5.96	0.95	0.285	1.23	(0.20)	(0.22)	-0.15
M6		6.84	0.96	0.30	1.26			0.0:
M7		7.8	0.96	0.31	1.27			0.0:

relations were derived using spectral types from the Michigan Catalogs (Houk 1978, 1982; Houk and Cowley 1975). The $(V-I)$ colors were from Cousins (1980*b*) for the bright stars and from Cousins (1980*a*), Bessell (1988*a*), and Weis (1987) (using Bessell and Weis 1987) for the nearby stars, in particular the M dwarfs.

X. Analysis of Passbands

Tracings of the filters of the AAO and MSO systems were kindly provided by D. A. Allen and A. R. Hyland. The MSO and AAO tracings were for a temperature of 77 K. We took the SAAO filters from Glass (1974), Johnson's filters from Johnson (1965*b*), and KPNO filters from Manduca and Bell (1979). The filter passbands of ESO and CIT were schematized from the published central wavelengths and half-widths. We decided to adopt the Kitt Peak mean summer prediction atmospheric transmissions of Manduca and Bell (1979) for wavelengths shortward of 2.6 μ and the measured KPNO atmospheric transmission of Ridgway for longer wavelengths. We divided the filter transmissions by the adopted atmospheric transmission to produce the initial passband estimates. Most of the recent filters have had passbands that fall completely within the atmospheric windows at *H* and *K*; however, the *J* filters all have their red cutoffs defined by the atmosphere.

We computed magnitudes and colors for several spectra, the Dreiling and Bell (1980) model of Vega, and a similar Bell model, the Labs and Neckel (1968) spectrum of the Sun, and the Strecker, Erickson, and Witteborn (1979) (SEW) spectra of the KM giants β Pegasi, α Ceti, β Andromedae, and α Tauri and their adopted flux for Vega. We extended the fluxes of the SEW stars to 1 μ by using the near-IR photometry of Wing (1967). The zero points were set by requiring that the Vega model have zero colors in all systems. The M-star spectrum enabled the differential variations of color or magnitude with spectral type to be examined. Blackbody fluxes were used in an initial examination, but the quantitative results differed from those using the stellar spectra. As the energy distribution of stars is nonblackbody, particularly in the *H* band, we accept the stellar-based comparisons as the more meaningful. When assessing the relative responses of the theoretical passbands of the different systems, we placed most weight on the passbands of MSO, AAO, and SAAO where we had the best filter data and the best observational comparisons. The *K* magnitudes were first compared, and small changes of the order of 100 Å were made to the effective wavelengths of the AAO, MSO, and SAAO to bring them to agreement with the observed color corrections. Similarly small corrections were made to ESO and CIT, but K_J required a much larger shift blueward. The $(J-K)$ colors were next compared. The MSO and SAAO colors were in good agreement and their *J* passbands adopted as being correct. Small shifts ($\sim$ 50 Å) were again made to the effective wavelengths of the other filters to produce matches with observational transformation coefficients. Johnson *J* required a large blueward shift this time to produce agreement. The *H* bands were similarly compared and adjusted using both $(H-K)$ and $(J-H)$ comparisons. The *H* band of the AAO was slightly blueshifted, but that of ESO required a large blue shift to produce agreement with the large observed color correction.

The synthetic $(K-L)$ and $(K-L')$ colors of MSO and AAO were compared. They indicated that $(K-L') = 1.29$ $(K-L')$, in reasonable agreement with the observed coefficient 1.33 from the AAO/CIT comparison. We adopted these unmodified basic responses as representing the 3.5-μ *L* and 3.8-μ *L'* passbands. The synthetic $(K-L')$ color of MSO indicated that $(K-L')_{\mathrm{AAO}} = 0.96\ (K-L')_{\mathrm{MSO}}$; unfortunately, standardized colors with the new MSO filter are not yet available for comparison. We took the AAO *M* response as adequate for adoptions as the *M* passband.

In Table IV are listed the adopted *J*, *H*, *K*, *L*, *L'*, and *M* passbands. These passbands could be better positioned in wavelength if spectrophotometry were available for some of the very red stars. In Figure 8, these adopted *J*, *H*, and *K* passbands and the assumed atmospheric transmission are plotted versus wavelength. Figure 9 similarly shows the *L*, *L'*, and *M* passbands and the atmospheric transmission.

Table V lists effective wavelengths of the passbands for Vega, the zero points used in the computation of the synthetic colors, and the adopted flux for a 0.03-mag star, derived from the Dreiling and Bell (1980) and the Bell (1987) model fluxes. The IR fluxes published for the Dreiling and Bell model are not detailed enough to show the Brackett lines, or the Brackett discontinuity; however, R. A. Bell kindly provided the detailed IR fluxes for a $T = 9650$ K, $\log g = 3.90$ model and these were used for the IR calibration.

Tüg, White, and Lockwood (1977) measured the flux for Vega (α Lyrae) at 5556 Å as being $F_\nu = 3.57 \times 10^{-20}$ erg cm^{-2} s^{-1} Hz^{-1}, with an estimated error of 1%–2%. The flux at 5450 Å (the effective wavelength of *V*) is 0.018 mag brighter than this. The *V* magnitude of α Lyr is about 0.03 mag; consequently, the zero-point constant in the equation: $m = -2.5 \log F_\nu + \text{constant}$ is $2.5 \log\{3.637\,E-20\} + 0.03 = -48.568$. With the slightly lower flux of Hayes and Latham (1975) the constant is -48.593. Dreiling and Bell (1980) derive a geometric dilution of $(1.62 \pm 0.03) \times 10^{16}$ (from the measured radius and parallax of Vega) to convert the model-atmosphere fluxes to observed fluxes for Vega at the Earth. Using a dilution of 1.62×10^{16} we derive a *V* magnitude of 0.04 or 0.016 from the scaled model-atmosphere fluxes. Given the uncertainties in the observations, this is good agreement; however, we will adopt the diluted model fluxes as

TABLE IV

Adopted Passbands

J	H	K	L	L'	M
1040 0.00	1460 0.00	1940 0.00	3040 0.00	3440 0.00	4440 0.00
1060 0.02	1480 0.15	1960 0.12	3080 0.02	3480 0.02	4480 0.13
1080 0.11	1500 0.44	1980 0.20	3120 0.09	3520 0.19	4520 0.34
1100 0.42	1520 0.86	2000 0.30	3160 0.38	3560 0.80	4560 0.30
1120 0.32	1540 0.94	2020 0.55	3200 0.30	3600 0.90	4600 0.39
1140 0.47	1560 0.98	2040 0.74	3240 0.50	3640 0.91	4640 0.50
1160 0.63	1580 0.95	2060 0.55	3280 0.61	3680 0.85	4680 0.44
1180 0.73	1600 0.99	2080 0.77	3320 0.41	3720 0.82	4720 0.16
1200 0.77	1620 0.99	2100 0.85	3360 0.50	3760 0.86	4760 0.35
1220 0.81	1640 0.99	2120 0.90	3400 0.61	3800 0.88	4800 0.33
1240 0.83	1660 0.99	2140 0.94	3440 0.70	3840 0.86	4840 0.37
1260 0.88	1680 0.99	2160 0.94	3480 0.85	3880 0.91	4880 0.44
1280 0.94	1700 0.99	2180 0.95	3520 0.88	3920 0.97	4840 0.44
1300 0.91	1720 0.95	2200 0.94	3560 0.84	3960 0.97	4880 0.37
1320 0.79	1740 0.87	2220 0.96	3600 0.84	4000 0.97	4920 0.37
1340 0.68	1760 0.84	2240 0.98	3640 0.84	4040 0.76	4960 0.23
1360 0.04	1780 0.71	2260 0.97	3680 0.86	4080 0.63	5000 0.07
1380 0.11	1800 0.52	2280 0.96	3720 0.65	4120 0.54	5040 0.03
1400 0.07	1820 0.02	2300 0.91	3760 0.19	4160 0.24	5080 0.00
1420 0.03	1840 0.00	2320 0.88	3800 0.04	4200 0.00	
1440 0.00	2340 0.84	3840 0.00			
	2380 0.75				
	2400 0.64				
	2440 0.10				
	2480 0.00				

TABLE V

Effective Wavelengths[1], Zeropoint Fluxes[2] and Magnitudes [3]

	V	J	H	K	L	L'	M	(M)
λeff	0.545	1.22	1.63	2.19	3.45	3.80	4.75	4.80
ZP	0.000	0.90	1.37	1.88	2.77	2.97	3.42	3.44
F_λ	3590	312	114	39.4	6.99	4.83	2.04	1.97
F_ν	3600	1570	1020	636	281	235	154	152

[1] In μm
[2] F_λ(10^{-15} W cm^{-2} μm^{-1}), F_ν(10^{-30} W cm^{-2} hz^{-1}) for a 0.03 magnitude star from Dreiling and Bell, and Bell Vega models for adopted passbands.
[3] Mag = $-2.5 \log\langle F_\nu\rangle - 66.08 - \mathrm{ZP}$

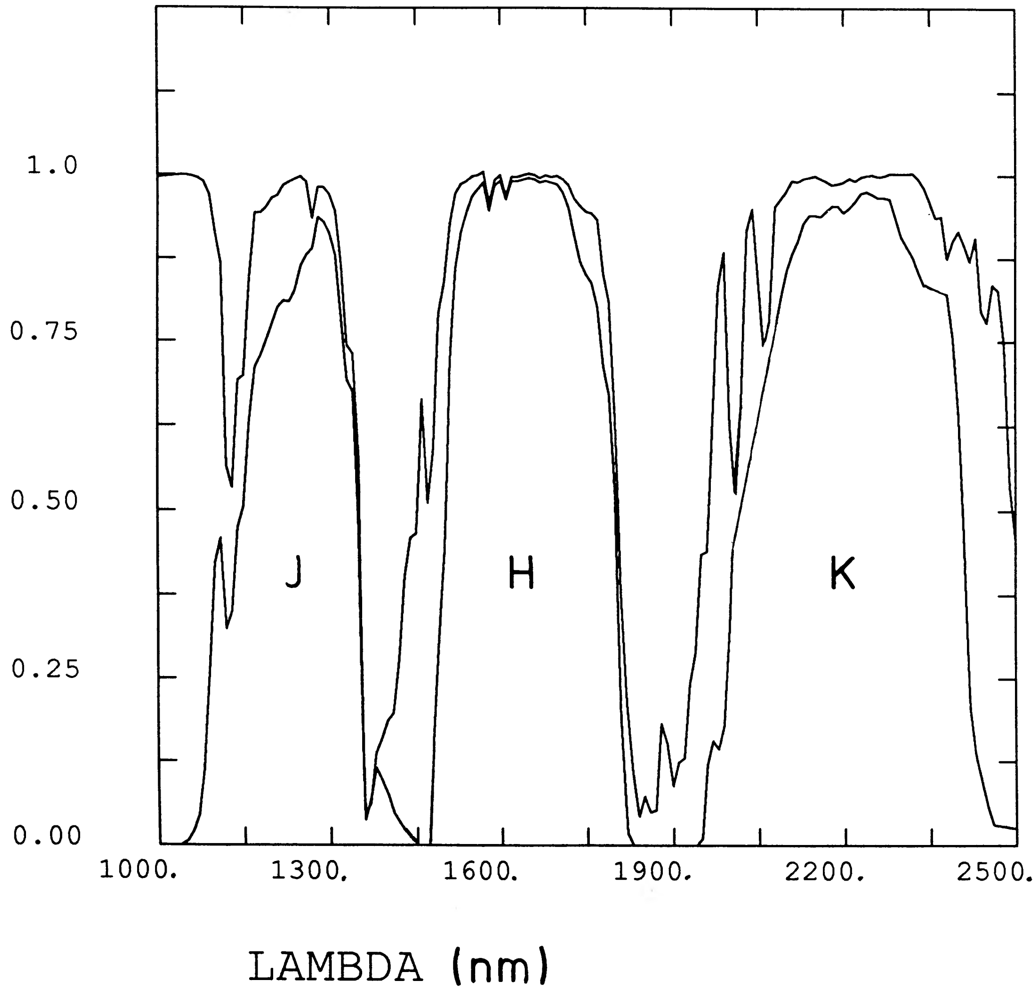

FIG. 8–Transmission of the atmosphere between 1 and 2.5 μm and adopted response function of J, H, and K.

appropriate to Vega and adjust the zero-point correction in the magnitude equation to produce a magnitude of 0.03 at V. The constant is then -48.58, for F_ν units of erg cm^{-2} sec^{-1} Hz^{-1}, and -66.08 for units of W cm^{-2} Hz^{-1}. Table VI lists the effective wavelengths of the various *JHK* systems, estimated as explained above.

In Table VII we give synthetic colors from various published fluxes and comparisons with measured colors or mean

TABLE VI

Effective Wavelengths (μm)

	John	MSO	AAO	SAAO	CIT	ESO	KPNO
				J			
Vega	1.222	1.221	1.198	1.216	1.246	1.213	1.221
Sun	1.235	1.227	1.206	1.222	1.250	1.219	1.227
β Peg	1.237	1.234	1.215	1.230	1.256	1.226	1.237
				H			
Vega	1.62	1.629	1.627	1.629	1.623	1.576	1.633
Sun	1.62	1.631	1.628	1.630	1.625	1.579	1.634
β Peg	1.63	1.639	1.636	1.639	1.633	1.593	1.642
				K			
Vega	2.209	2.188	2.205	2.205	2.217	2.184	2.209
Sun	2.209	2.188	2.207	2.205	2.217	2.185	2.209
β Peg	2.202	2.182	2.200	2.199	2.212	2.176	2.202

TABLE VII

Comparison between Measured and Computed Colors

	B-V	V-I	V-K	J-H	H-K	J-K	K-L	K-L'	K-M
L and N Sun	0.66	0.72	1.52	0.333	0.043	0.376	0.043	0.051	0.012*
Solar analog	0.66	0.71	1.53	0.33	0.055	0.385	0.05	0.05	0.01
SEW Vega				-0.013	0.006	-0.007	0.020	0.023	0.021
Ten Vega				0.011	0.033	0.044	0.027	0.037	0.060
DB model				-0.009	0.013	0.004	-0.009	-0.009	-0.011
SEW α Tau K5.7III				0.81	0.18	0.98	0.15	0.17	-0.12
Table 3				0.81	0.18	0.98	0.12	0.16	-0.09
Lee, THR				0.75	0.22	0.97	0.16		-0.07
SEW β And M0.5III				0.86	0.19	1.05	0.14	0.13	-0.14
Table 3				0.84	0.19	1.03	0.13	0.17	-0.09
Lee, MKO				0.82	0.20	1.02	0.23	0.19	-0.07
SEW α Cet M1.7III				0.83	0.26	1.09	0.15	0.19	-0.12
Table 1				0.86	0.21	1.07	0.15	0.19	-0.09
Glass, Lee, THR				0.85	0.22	1.07	0.10		-0.12
SEW β Peg M3.2II var				0.92	0.22	1.14	0.16	0.20	-0.11
Table 1				0.90	0.235	1.13	0.16	0.20	-0.07
Lee, MKO				0.91	0.25	1.16	0.20	0.17	-0.02

* Labs and Neckel IR flux is from a model. The K-M color from that flux is 0.061. The color listed here was derived from the difference between the model flux and the measured flux. See Section 10 for details.

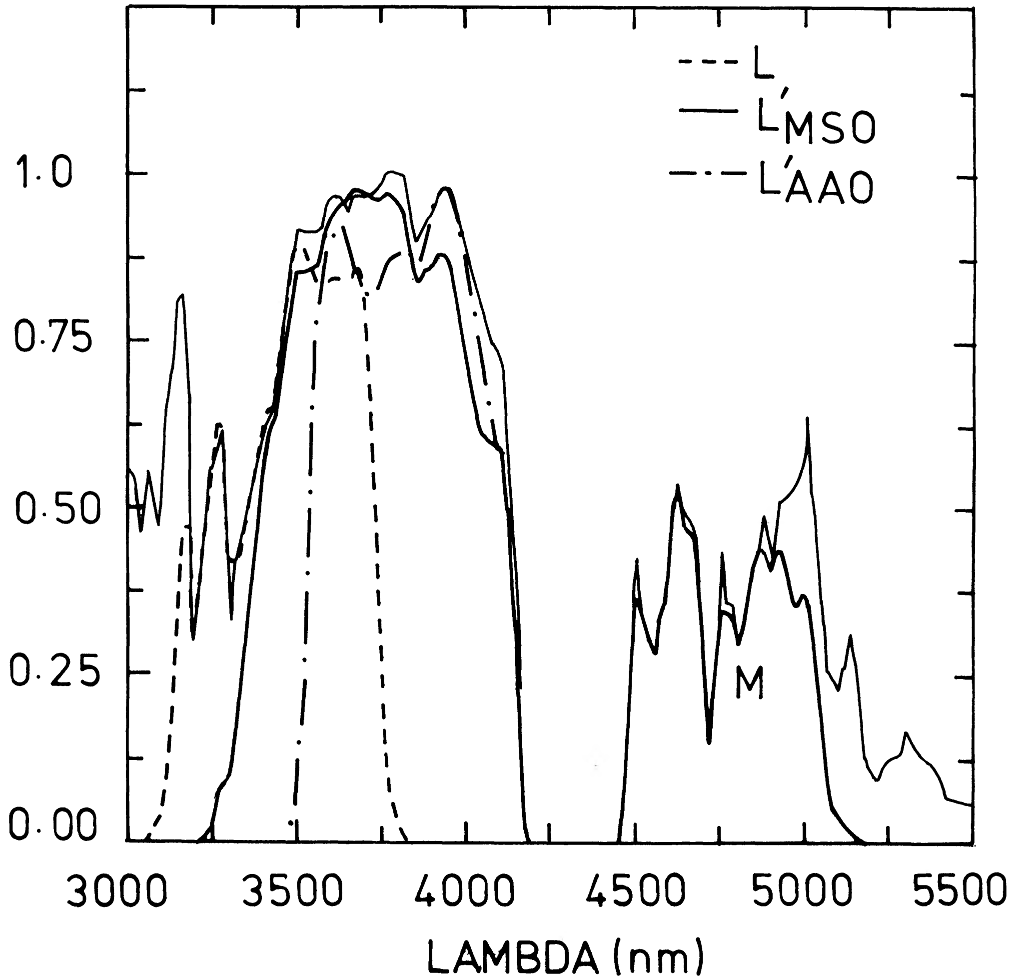

FIG. 9–Transmission of the atmosphere between 3 and 5.5 μm and adopted response function of L, L'(MSO and MKO) and L'(AAO), and M.

colors for similar spectral types. In particular we compare solar-type star colors with synthetic colors derived from the Labs and Neckel (1968) fluxes for the Sun. Bessell and Norris (1984) suggest that the mean $(V-I)$ color of solar analogs is 0.71, and the corresponding intrinsic IR colors from data in Table III are also given in Table VII. The agreement is excellent in all colors. We must, however, comment on the solar IR fluxes used in the computation. The IR spectrum adopted for the Sun by Labs and Neckel is that for a model, and it is clear from a comparison of model solar fluxes and observed solar fluxes shown by Labs and Neckel (1972) (Fig. 3 in that paper) that the model fluxes do not include the effects of CO absorption. Inspection of the $(K-M)$ versus $(V-K)$ diagram above (Fig. 7) shows that the observed $(K-M)$ colors *already* begin to show a turndown due to CO absorption in the late-F stars. Using the Labs and Neckel figure, we adjusted the model flux to produce the measured CO depression and computed the solar M magnitudes. The tabluated Labs and Neckel IR continua gave $(K-M) = 0.061$; the adjusted continua gave $(K-M) = 0.012$. (This 6% difference does not appear to have been taken into account by Campins, Rieke, and Lebofsky (1985) in their calibration of M photometry.) It is gratifying that the adopted fluxes for Vega lead to colors for a solar analog that are within 1% of the colors computed from solar fluxes between 0.3 μ and 5 μ. Uncertainties due to hydrogen lines in Vega and CO lines in the Sun probably account for the differences at H. There are other versions for the IR flux of Vega that are also of interest. These are by Strecker *et al.* (1979, SEW), Dreiling and Bell (1980), and Blackwell *et al.* (1986) (Ten). The latter fluxes were measured broadband fluxes relative to a standard source. The IR colors computed from these fluxes are also given in Table VII, in comparison to zero colors for the adopted model fluxes. Now the zero points of the homogenized photometric system were set by ensuring that stars with $(V-I)$ and $(V-K)$ values of zero (i.e., average A0 stars) have zero IR colors, so that even were Vega to have an IR excess, it would not necessarily affect this procedure unless all A0 stars had a similar excess. However, Vega does have colors close to zero in all of the systems and this suggests that the apparent IR excess measured by Blackwell between 3 μ and 5 μ cannot be real.

Our flux calibration for the *JHKLM* system is similar to that of Campins *et al.* (1985) based on their solar analogs;

however, these authors have used different effective wavelengths than our analysis indicates for the *J* and *M* bands in particular which will result in a slightly different model flux, and they apparently make no adjustment for the CO depression in the *M* band of the G dwarfs as compared to the solar model fluxes of Labs and Neckel.

The synthetic colors derived for some of the bright SEW KM stars discussed above are compared with intrinsic colors for the relevant spectral types from Table III and with colors from Johnson *et al.* (1966) (LPL4), and Sinton and Tittemore (1984) (MKO) for $(K-L')$, $(K-M)$ of β Peg and β And, and Thomas *et al.* (1973) for $(K-M)$ for α Tau and α Cet. Given the uncertainties involved the agreement is excellent, except in $(K-M)$ where there appears to be a small systematic difference, which could easily be accounted for by atmospheric absorption effects in *M*.

As a result of this analysis, we feel that we understand the interrelations of the various IR photometric systems and feel confident to compute synthetic colors from spectra. However, a better analysis of the passbands will be possible when accurate IR spectrophotometry for a variety of objects with known broad-band colors (in particular those heavily reddened stars used to better explore the different IR systems) is available. We urge that such observations be made in *J*, *H*, *K*, *L*, and *M* windows and we encourage the authors of grids of model atmospheres to publish IR fluxes and/or broad-band *JHKL* colors to supplement the available *UBVRI* and *uvby* colors.

We would like to thank David Allen, Peter McGregor, and Harry Hyland for helpful discussions and advice and Roger Bell for kindly providing the infrared fluxes of an A0 star model. The referee also made helpful comments. It is appropriate to record our gratitude to those who have provided us with sensitive IR systems and precise standards, so that accurate measurements in the IR are now a matter of course.

APPENDIX

A. *Spectral Type Versus Color Relations*

Figures A1 and A2 are plotted with color data from Cousins (1980*a*,*b*) and spectral types from Houk and Cowley (1975) and Houk (1978, 1982). They indicate the possible range in color for any spectral type.

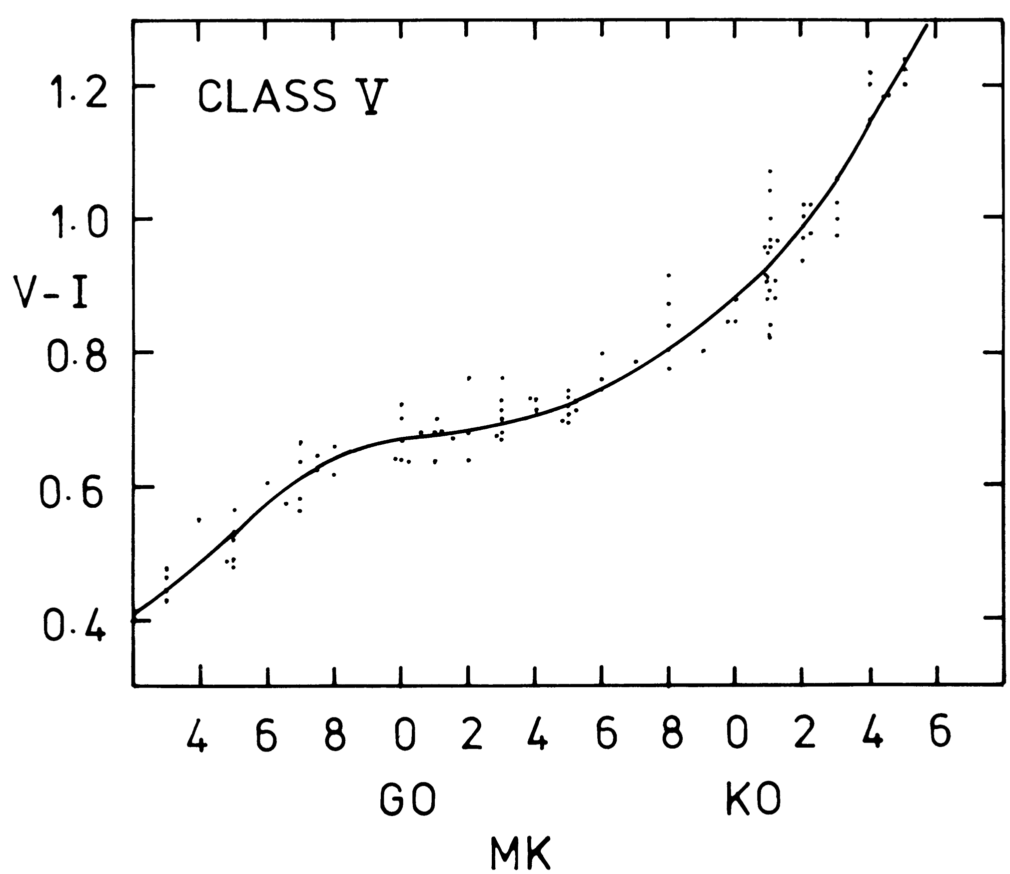

FIG. A1–$(V-I)$ versus MK spectral type for G–K dwarfs.

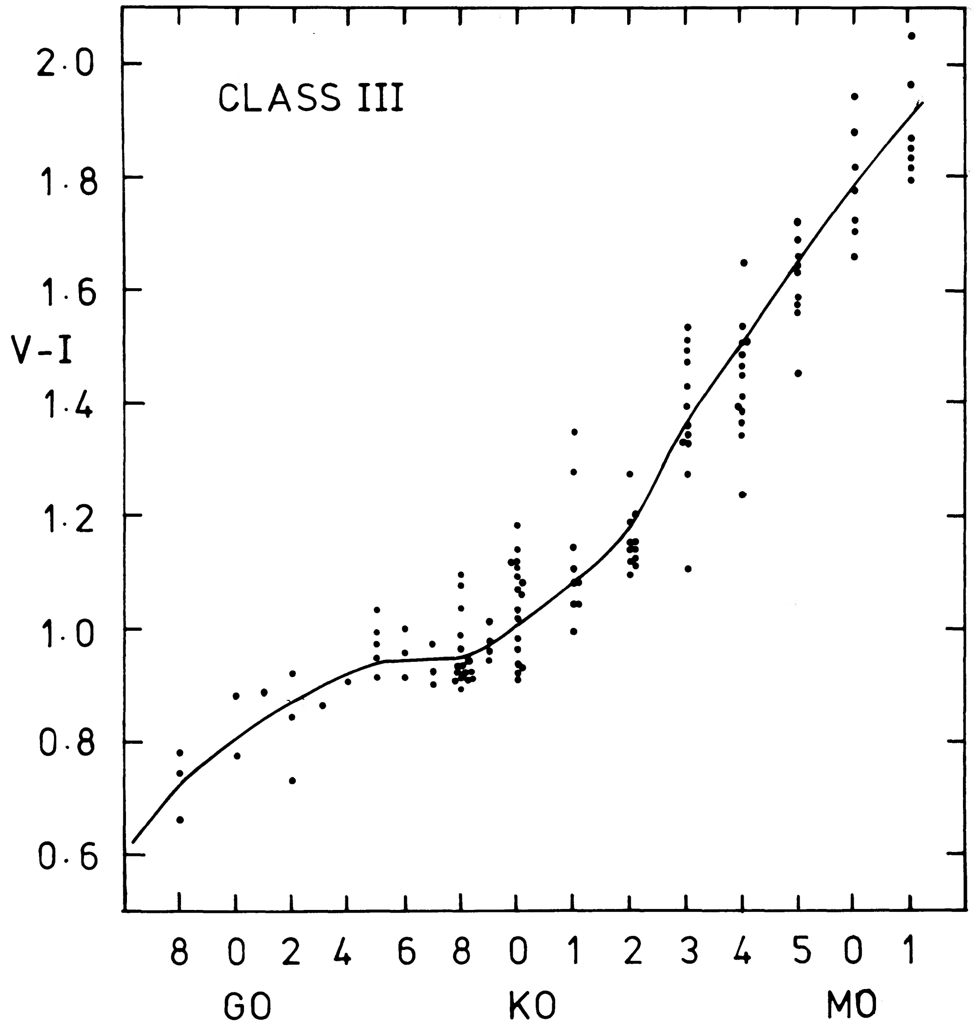

FIG. A2–$(V-I)$ versus MK spectral type for G–K giants.

B. *Reddening Relations for Various Colors*

The effect of interstellar reddening on the colors of stars has been discussed, for example, by Lee (1970), Becklin *et al.* (1978), Jones and Hyland (1980), Whittet and van Breda (1980), and Rieke and Lebofsky (1985). We adopt from these papers, and from Dean, Warren, and Cousins (1978), the following relations.

$$E(V-I) = 1.25\,E(B-V) \qquad A_V = 3.12\,E(B-V)$$
$$E(V-K) = 2.78\,E(B-V) \qquad A_K = 0.34\,E(B-V)$$
$$E(J-H) = 0.37\,E(B-V)$$
$$E(H-K) = 0.19\,E(B-V)$$
$$E(K-L) = 0.15\,E(B-V)$$
$$E(K-M) = 0.24\,E(B-V)$$

The ratio of $A_V/E(B-V)$ is higher in some dark cloud regions, such as Orion (see, e.g., Whittet and van Breda 1980).

C. *Atmospheric Extinction*

Manduca and Bell (1979) have discussed in great detail the expected atmospheric extinction in the J, H, and K bands. Glass (1985) has summarized the results. In normal differential photometry, extinction derived between 1 and 2 air masses in the usual way is adequate, although in J there can be systematic differences in extinction between A and M stars, particularly from summer to winter, or on humid nights, or day to night, because of the more significant H_2O absorption in the J band. Observing program and standard stars over the same small range in air mass and using mean extinction is usually adequate, although on nights when the humidity changes, the zero-point corrections do vary. In particular, photometry in the original L band and the M band often suffers from the absorption varying through the night as the humidity changes. Obviously some sites are much worse than others. The most important effects concern the absolute calibration of photometry, when the extinction correction to zero air mass is needed to compare stellar measurements with a laboratory standard source. Manduca and Bell show that this true extinction correction can be from 1.3 to 1.8 times the extinction derived between 1 and 2 air masses. (The passbands derived in this paper contain the effect of approximately 1.2 air masses of a standard KPNO atmosphere.) If absolute photometry is required, then narrow-band filters which completely avoid the H_2O features should be used.

Although extinction coefficients tend to be very site and season dependent it is of interest to show some mean measured extinction coefficients (in mag air mass^{-1}) at the AAO (Allen 1981).

J	0.12 – 0.18,	~ 0.08 – 0.12 (MSO filter)
H	0.06 – 0.10	
K	0.10 – 0.15	
L'	0.11 – 0.16	

Mean extinction coefficients at Mauna Kea (Sinton and Tittemore 1984) are

$$L' \; 0.09 \pm 0.05$$
$$M \; 0.22 \pm 0.07 \; .$$

D. *IR Colors of Long-Period Variables, Carbon Stars, and Late-Type Supergiants*

Tables II and III contain the intrinsic colors of normal, near-solar composition, class III giants and dwarfs. Some stars, such as supergiants, carbon stars, and long-period variables, have more extreme colors. This is mainly due to molecular blanketing from CO and CN in supergiants, CO, CN, C2, and HCN in carbon stars, and TiO, VO, CO, and H_2O in M long-period variables (LPVs), although the cooler continuum temperatures also redden the colors. In Figure A3 we have

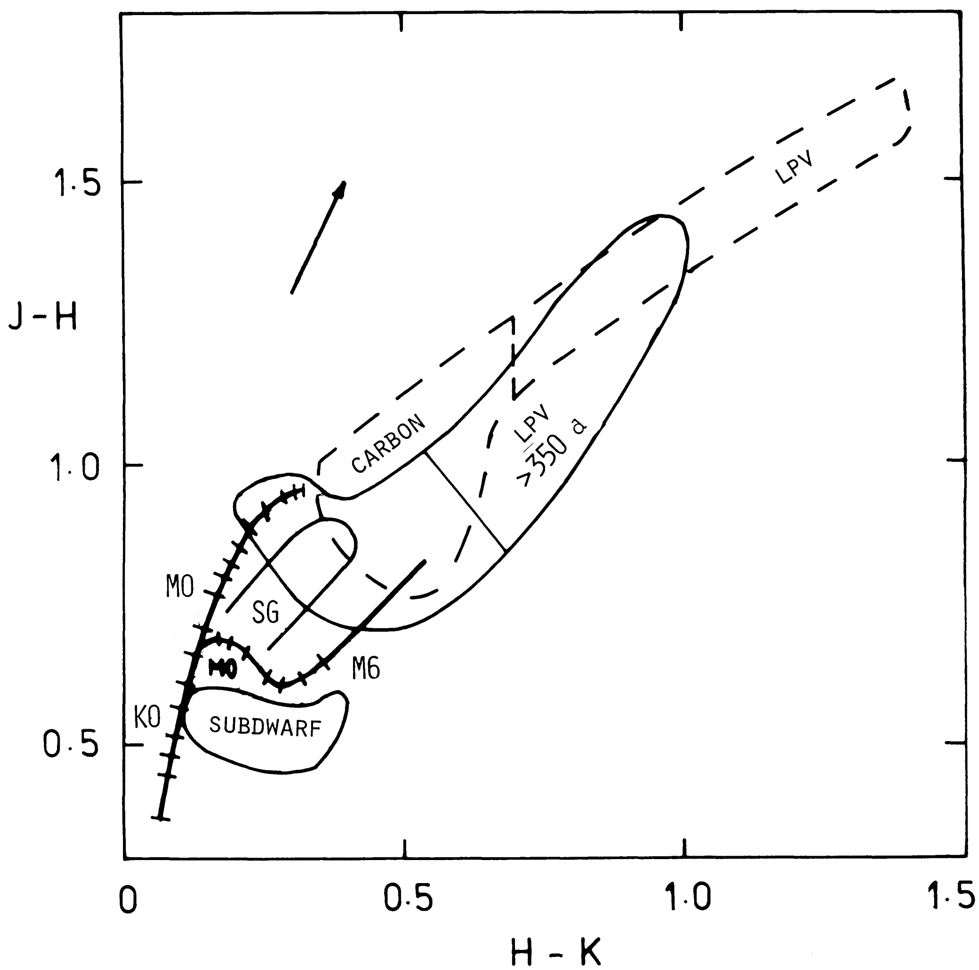

FIG. A3–The $(J-H)$ versus $(H-K)$ diagram showing schematically the regions occupied by G5 to M6 dwarfs and giants, SR and LPV carbon stars, and SR and LPV M7–M10 AGB stars. The arrow indicates the direction of interstellar reddening.

schematically plotted the areas in the two-color diagram defined by typical stars. The data were taken from Bessell, Wood, and Lloyd Evans (1983), Magellanic Cloud carbon stars; Walker (1980), galactic carbon stars; Wood and Bessell (1983), solar neighborhood and galactic-center M LPVs; Wood, Bessell, and Paltoglou (1985), Magellanic Cloud M and C LPVs; and Lee (1970), supergiant M stars.

The dashed lines enclose the area occupied by most carbon-rich stars; the carbon LPVs lie within the right-hand-end division of the box. The M-type (oxygen-rich) LPVs fall within the area defined by the continuous line; the metal-poor Miras (47 Tucanae-like) overlap part of the normal giant sequence, the solar-composition semiregular and short-period variables form a continuation of the giant sequence, and the LPVs with periods greater than ~ 250 days occupy the right-hand edge of the box, which overlaps the carbon LPVs. The supergiant M stars lie in a region below, and to the right of, the giant sequence. The metal-poor M dwarfs (subdwarfs) lie below the dwarf line.

E. *Absolute Calibration of Fluxes*

We chose to adopt a theoretical flux calibration for Vega (Dreiling and Bell 1980; Bell 1987). This was done because it proved a reliable method for the optical and near-IR spectral region. However, recently Blackwell *et al.* (1986) have discussed the implications of absolute flux measurements of Vega made at Tenerife, which indicate that Vega is redder at K, L, and M than the model fluxes predict. The comparisons made in this paper suggest that Vega cannot be as red as the Blackwell measurements suggest. More detailed discussions are given in Section X.

F. *Bolometric Corrections for Late-Type Stars*

Bolometric corrections have been derived by Johnson (1966), Lee (1970), and Frogel, Persson, and Cohen (1981). More recently, Bessell and Wood (1984) have rederived BCs to I_C, H, and K for late-type giants in the Galaxy and Magellanic Clouds. Veeder (1974) and Reid and Gilmore (1984) have derived BCs for M dwarfs.

REFERENCES

Allen, D. A. 1981, *IRPS Users Guide*, Anglo-Australian Observatory.

Allen, D. A., and Cragg, T. A. 1983, *M.N.R.A.S.*, **203**, 777.

Becklin, E. E., Matthews, K., Neugebauer, G., and Willner, S. P. 1978, *Ap. J.*, **220**, 831.

Bell, R. A. 1987, private communication.

Bessell, M. S. 1988*a*, *Astr. Ap.*, submitted.

———. 1988*b*, *Ap. J.*, submitted.

Bessell, M. S., and Norris, J. E. 1984, *Ap. J.*, **285**, 622.

Bessell, M. S., and Weis, E. W. 1987, *Pub. A.S.P.*, **99**, 642.

Bessell, M. S., and Wood, P. R. 1984, *Pub. A.S.P.*, **96**, 247.

Bessell, M. S., Brett, J., Scholz, M., and Wood, P. R. 1985, in *IAU Symposium 111, Calibration of Fundamental Stellar Quantities*, ed. D. S. Hayes, L. E. Pasinetti, and A. G. Davis Phillip (Dordrecht: Reidel), p. 539.

———. 1988*a*, *Astr. Ap.*, submitted.

———. 1988*b*, *Astr. Ap.*, submitted.

Bessell, M. S., Wood, P. R., and Lloyd Evans, T. 1983, *M.N.R.A.S.*, **202**, 59.

Blackwell, D. E., Booth, A. J., Petford, A. D., Leggett, S. K., Mountain, C. M., and Selby, M. J. 1986, *M.N.R.A.S.*, **221**, 427.

Boeshaar, P. C. 1976, Ph.D. dissertation, Ohio State University.

Brett, J. M. 1988, Ph.D. dissertation, Australian National University.

Campins, H., Rieke, G. H., and Lebofsky, M. J. 1985, *A.J.*, **90**, 896.

Carter, B. S. 1984, M.Sc. thesis, University of Cape Town.

Cousins, A. W. J. 1980*a*, *South African Astr. Obs. Circ.*, **1**, 166.

———. 1980*b*, *South African Astr. Obs. Circ.*, **1**, 234.

Dean, A. R., Warren, P. R., and Cousins, A. W. J. 1978, *M.N.R.A.S.*, **183**, 569.

Dreiling, L. A., and Bell, R. A. 1980, *Ap. J.*, **241**, 736.

Elias, J. H., Frogel, J. A., and Humphreys, R. M. 1985, *Ap. J. Suppl.*, **57**, 91.

Elias, J. H., Frogel, J. A., Hyland, A. R., and Jones, T. J. 1983, *A.J.*, **88**, 1027.

Elias, J. H., Frogel, J. A., Matthews, K., and Neugebauer, G. 1982, *A.J.*, **87**, 1029.

Engels, D., Sherwood, W. A., Wamsteker, W., and Shultz, G. V. 1981, *Astr. Ap. Suppl.*, **45**, 5.

Frogel, J. A., Persson, S. E., and Cohen, T. G. 1981, *Ap. J.*, **246**, 842.

Glass, I. S. 1974, *Mon. Notes Astr. Soc. Sth. Afr.*, **33**, 53, 71.

———. 1983, *Mon. Notes Astr. Soc. Sth. Afr.*, **43**, 43.

———. 1985, *Irish A.J.*, **17**, 1.

Hayes, D. S., and Latham, D. W. 1975, *Ap. J.*, **197**, 593.

Houk, N. 1978, *Michigan Catalogue of Two-Dimensional Spectral Types for the HD Stars*, Vol. **2** (Ann Arbor: University of Michigan Department of Astronomy).

———. 1982, *Michigan Catalogue of Two-Dimensional Spectral Types for the HD Stars*, Vol. **3** (Ann Arbor: University of Michigan Department of Astronomy).

Houk, N., and Cowley, A. 1975, *Michigan Catalogue of Two-Dimensional Spectral Types for the HD Stars*, Vol. **1** (Ann Arbor: University of Michigan Department of Astronomy).

Hyland, A. R., and McGregor, P. J. 1986, private communication.
Johnson, H. L. 1965*a*, *Ap. J.*, **141**, 925.
———. 1965*b*, *Common Lunar Planet. Lab.*, **3**, 73.
Johnson, H. L. 1966, *Ann Rev. Astr. Ap.*, **4**, 193.
Johnson, H. L., MacArthur, J. W., and Mitchell, R. E. 1968, *Ap. J.*, **152**, 465.
Johnson, H. L., Mitchell, R. I., Iriate, B., and Wisniewski, W. Z. 1966, *Comm Lun. Planet. Lab.*, **4**, 99.
Jones, T. J., and Hyland, A. R. 1980, *M.N.R.A.S.*, **192**, 359.
———. 1982, *M.N.R.A.S.*, **200**, 509.
Koorneef, J. 1983*a*, *Astr. Ap. Suppl.*, **40**, 1.
———. 1983*b*, *Astr. Ap.*, **128**, 84.
Labs, D., and Neckel, H. 1968, *Zs. f. Ap.*, **69**, 1.
———. 1972, *Solar Phys.*, **22**, 64.
Lee, T. A. 1970, *Ap. J.*, **162**, 217.
Manduca, A., and Bell, R. A. 1979, *Pub. A.S.P.*, **91**, 848.
Persson, S. E., Aaronson, M., and Frogel, J. A. 1977, *A.J.*, **82**, 729.
Reid, I. N., and Gilmore, G. F. 1984, *M.N.R.A.S.*, **206**, 19.
Ridgway, S. T., Joyce, R. R., White, N. M., and Wing, R. F. 1980, *Ap. J.*, **235**, 126.
Rieke, G. H., and Lebofsky, M. J. 1985, *Ap. J.*, **288**, 618.
Scholz, M. 1985, *Astr. Ap.*, **145**, 251.
Sinton, W. M., and Tittemore, W. C. 1984, *A.J.*, **89**, 1366.
Stauffer, J. R., and Hartman, L. W. 1986, *Ap. J. Suppl.*, **61**, 1986 (SH).
Strecker, D. W., Erickson, E. F., and Witteborn, F. C. 1979, *Ap. J. Suppl.*, **41**, 501.
Thomas, J. A., Hyland, A. R., and Robinson, G. 1973, *M.N.R.A.S.*, **165**, 201 (THR).
Tüg, H., White, N. M., and Lockwood, G. W. 1977, *Astr. Ap.*, **61**, 679.
Veeder, G. J. 1974, *A.J.*, **79**, 1056.
Walker, A. R. 1980, *M.N.R.A.S.*, **190**, 543.
Wamsteker, W. 1981, *Astr. Ap.*, **97**, 329.
Weis, E. W. 1987, *A.J.*, **93**, 451.
Whittet, D. C. B., and van Breda, I. G. 1980, *M.N.R.A.S.*, **192**, 467.
Wing, R. F. 1967, Ph.D. dissertation, University of California, Berkeley.
Wood, P. R., and Bessell, M. S. 1983, *Ap. J.*, **265**, 748.
Wood, P. R., Bessell, M. S., and Paltoglou, G. 1985, *Ap. J.*, **290**, 477.